Unusual Premonsoon Eddy and Kelvin Wave Activities in the Bay of Bengal During Indian Summer Monsoon Deficit in June 2009 and 2012

Subhra Prakash Dey, Mihir K. Dash, Pranab Deb, Dhrubajyoti Samanta, Rashmi Sharma, Rakesh Mohan Gairola, Raj Kumar, and Prem Chand Pandey

***Abstract*— An investigation of the eddy and coastal Kelvin wave activities in the Bay of Bengal (BoB) is carried out during premonsoon season in two years of Indian summer monsoon deficit in June (2009 and 2012), occurred in the recent warming hiatus period. Using altimeter observations, our study reveals that over the northern BoB cyclonic eddy kinetic energy is reduced by 35% and 50% from the climatology during premonsoon seasons in 2009 and 2012, respectively, while the cyclonic eddy area is reduced by 18% and 24%, respectively. A concurrent reduction is observed in the first upwelling Kelvin wave (uKW) activities in the eastern equatorial Indian Ocean as well as in the coastal BoB for these years. The reduction in the generation of the first uKW in the eastern equatorial Indian Ocean is attributed to the westerly wind anomalies in January–March of these years. Additionally, meridional wind stress anomalies during March–April in these years are found to be southerly, causing anomalous coastal downwelling in the eastern rim of BoB. This coastal downwelling blocks the propagation of the first uKW. The decrease in the first uKW activities in the coastal waveguide of the BoB reduces the radiation of upwelling Rossby waves, thereby decreasing the cyclonic eddy activities in the northern BoB. The results from this letter could be helpful for further understanding of upper ocean mixing processes in the BoB during monsoon deficit years.**

***Index Terms*— Altimetry, Bay of Bengal (BOB), eddy activity, Indian summer monsoon (ISM), Kelvin wave.**

I. Introduction

THE Bay of Bengal (BoB) is a semienclosed bay located in the northeastern part of the Indian Ocean. Upper ocean processes in the BoB play a vital role in the onset and progression of South Asian and Indian summer monsoon (ISM). Sea surface warming in the central BoB during premonsoon season (March–May) triggers the onset of South Asian monsoon [1]. The frequency and lifetime of low-pressure areas in ISM season (June–September) are positively correlated with the premonsoon sea surface temperature (SST) over the BoB [2]. However, the BoB in general and the northern bay, in particular, plays a significant role in the monsoon rainfall through the formation of the low-pressure systems [3]. Despite the significant control of upper ocean behavior on the ISM rainfall, most monsoon prediction models have a poor representation of upper ocean mixing [3]. Therefore, the study of mesoscale eddies, which control the upper ocean mixing, over the BoB is necessary.

Mesoscale eddies in the ocean are the spatial structures similar to coherent vortices of 2-D turbulence [4] and are responsible for the vertical mixing, upper surface thermal structure, and transport of heat between different parts of the ocean. Also, they can locally affect the near-surface wind, cloud properties, and rainfall, and thereby the larger low-pressure systems [5]. The coastal Kelvin wave in the eastern rim of BoB radiates its energy toward the interior bay through eddy shedding [6]. Further, using nine years of altimetry data, Cheng *et al.* [7] found that eddy train originated from the coastal waveguide of BoB contributes to the intraseasonal variability of sea level and thermal properties in the central bay.

During the recent warming hiatus period (1999–2013) [8], the upper ocean heat content in the Indian Ocean showed an increase [9]. The increase in heat content is attributed to the strengthening of Walker circulation and a subsequent increase in heat advection toward the Indian Ocean by Indonesian throughflow [9]. An increase in rainfall is noted during the hiatus period compared to prehiatus time over the western Pacific and the western Indian Ocean, while a decrease is evident over the east Asia [8]. This hiatus period has observed two severe June ISM deficit years, in 2009 and 2012, with more than 20% rainfall deficiency (see Table S1 in the Supplementary Material).

This letter investigates the premonsoon eddy activity in tandem with Kelvin wave activities using altimetric observations over the BoB in two June ISM deficit years (2009 and 2012). The possible physical mechanisms behind such anomalous eddy and Kelvin wave activities are also explored by analyzing the local winds over the BoB and the remote winds over the equatorial Indian Ocean (EIO; (5°S–5°N, 40°E–100°E)).

II. Data and Methodology

We used merged and gridded daily sea level anomaly (SLA) and the geostrophic current data, from

This work was supported in part by the Space Applications Centre, ISRO, India. *(Corresponding author: Mihir K. Dash.)*

S. P. Dey, M. K. Dash, and P. C. Pandey are with the Centre for Oceans, Rivers, Atmosphere and Land Sciences, IIT Kharagpur, Kharagpur 721302, India (e-mail: mihir@coral.iitkgp.ernet.in).

P. Deb is with the Climatic Research Unit, University of East Anglia, Norwich NR4 7TJ, U.K.

D. Samanta is with the Asian School of the Environment, Nanyang Technological University, Singapore 639798.

R. Sharma, R. M. Gairola, and R. Kumar are with the Atmospheric and Oceanic Science Group, Space Applications Centre, Ahmedabad 380015, India.

1994 to 2015, available from the archiving, validation, and interpretation of satellite oceanographic data (AVISO, htttp://www.aviso.oceanobs.com). These products are constructed by merging multisatellite (TOPEX/Poseidon, European Remote Sensing Satellite 1/2, Jason 1, Jason 2, Envisat, etc.) data sets. These data sets are available on a Cartesian grid of 0.25° × 0.25° spatial resolution derived from a Mercator grid through linear interpolation. Also, we use daily surface wind stress and wind field, from 1994 to 2015, available from the Modern-Era Retrospective Analysis for Research and Applications (MERRA) reanalysis product. For eddy detection, we used the Okubo–Weiss method [10] that showed potentiality to detect eddies over the Mediterranean Sea, the Tasman Sea, and the Gulf of Alaska [11]. After the identification of cyclonic and anticyclonic eddies, their effective area is calculated separately by integrating the area of simply connected grid boxes inside a vortex. The area of the vortex is given as

$$A = \sum_{n=1}^{N_{gp}} A_n \tag{1}$$

where A_n is the area of nth grid box, calculated considering the earth to be spherical, and N_{gp} represents the number of simply connected grid boxes inside a vortex. Total surface eddy kinetic energy of a vortex is calculated using the following equation:

$$E = \frac{1}{2} \sum_{i=1}^{N_{gp}} \left(u_i^2 + v_i^2 \right) \tag{2}$$

where u_i and v_i are the zonal and meridional components of geostrophic velocity, respectively.

III. Results and Discussions

In this section, we first examine eddy activity over the northern BoB in the premonsoon period of 2009 and 2012. Then, activities of equatorial Kelvin waves and coastal Kelvin waves over the BoB are studied in the context of eddy activity. Finally, their dependence on equatorial winds and local winds over the BoB is explored.

A. Eddy Activity in the Northern BoB

Fig. 1 compares the area integrated daily eddy kinetic energy (EKE) and eddy area (hereafter represented as eddy area) for the cyclonic eddies in the northern BoB (14°N–23°N and 78°E–99°E) for 2009 and 2012 against the climatology considering the altimetric era: 1994–2015. Generally, both the cyclonic EKE and eddy area peaks in May and then decreases in June. Cyclonic EKE is found to be significantly reduced (less than the lower bound of 95% confidence level) from mid-April to end of May of 2009 [Fig. 1(a)]. A similar reduction is noticed in cyclonic eddy area from mid-April to the first week of May [Fig. 1(c)]. On an average, cyclonic EKE and eddy area are found to decrease by 35% and 18%, respectively, from their climatological values during the span of one month (15 April–15 May) in 2009. The year 2012 also experienced a significant reduction in

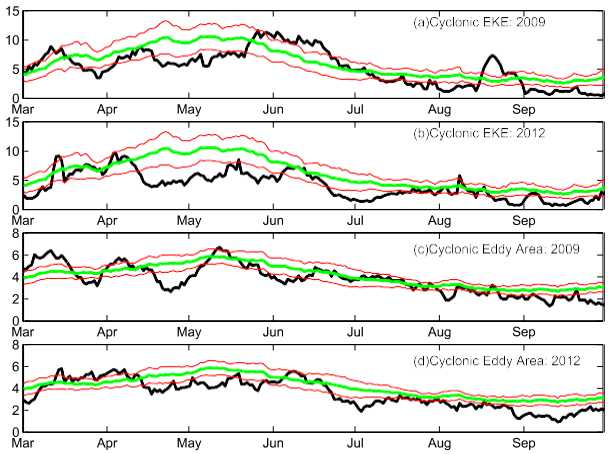

Fig. 1. Black lines represent total cyclonic EKE (in m^2s^{-2}) in the northern BoB (14°N–23°N 78°E–99°E) for (a) 2009 and (b) 2012, and cyclonic eddy area (in the unit of 10^4 km^2) over the same region for (c) 2009 and (d) 2012. The green curves represent the climatology considering the period 1994–2015. The magenta lines show 95% confidence levels from the average.

cyclonic EKE and eddy area during mid-April to the first week of June [Fig. 1(b) and (d)]. On average, 50% reduction of cyclonic EKE and 24% reduction of cyclonic eddy area are noticed during 15 April–15 May. On the other hand, the analysis of anticyclonic eddy activity (see Fig. S1 in the Supplementary Material) does not show any systematic signal. Naturally, the question arises, what causes the cyclonic eddy activities to reduce? Eddies in this region may occur due to local wind forcing, internal turbulence, and the remote forcing from the equator through coastal Kelvin waves and subsequently radiated Rossby waves. Due to high Reynold's number (order of 10^8 [12]), any current in the ocean can produce some turbulent eddies [13]. Since currents in the bay are weak, the vortices generated due to the turbulence of the system are mostly negligible. Moreover, these types of eddies always remain present in the bay and do not add extra value to the systematic seasonal or intraseasonal variability. Fig. 2 compares the daily wind stress curl averaged over the north-central bay (14°N–19°N and 87°E–93°E) during March–September of 2009 and 2012 against the composite of all 22 years. The composite plot shows that wind stress curl does not vary much over the whole period (March–September). In 2009, wind stress curl remained within one standard deviation limit [Fig. 2(a)] except for some special events. Two severe cyclonic storms [Bijli (14–16 April) and Aila (23–26 May)] occurred during the premonsoon period of this year, which are reflected as peaks in averaged wind stress curl over the region [Fig. 2(a)]. Another peak in wind stress curl is observed in the first week of June. This represents the presence of deep depression over the bay. During 2012, no signature of such weather systems is seen over the region in the premonsoon period and in the month of June. Frequent fluctuations in wind stress curl are observed during monsoon time, but most of the time they are within the error limits, i.e., one-sigma levels and last for very short period. This suggests that wind stress curl is

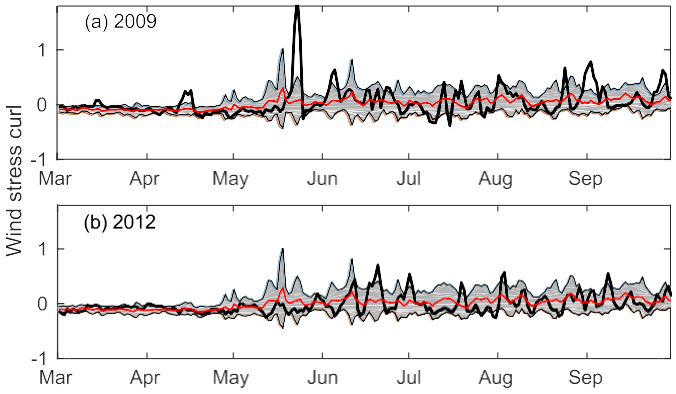

Fig. 2. Averaged wind stress curl (in 10^{-6} Nm^{-3}) over the north-central BoB (14°N–19°N, 87°E–93°E) for the June ISM deficit years (a) 2009 and (b) 2012 (black curves). The red curves represent the composite value of the same. The gray shades indicate one standard deviation limit.

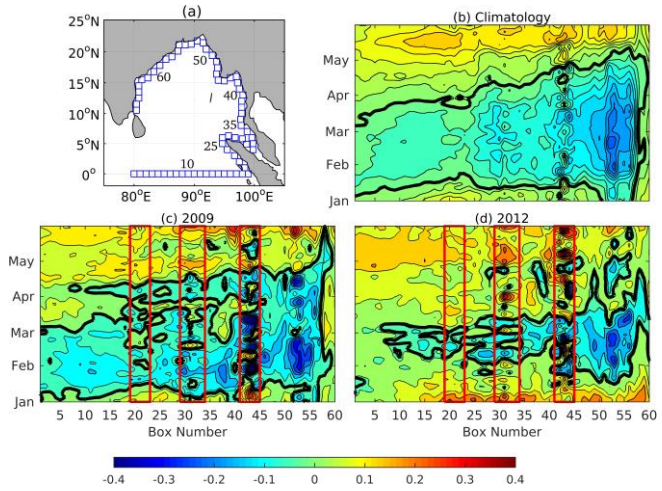

Fig. 3. (a) Distribution of 1° ✖° boxes along the equatorial (starting from 80°E) and coastal waveguides in the BoB. Time-box number plots of SLA for (b) climatology and the years (c) 2009 and (d) 2012. Thick lines represent the zero contour. The red vertical rectangles show the discontinuities in the SLA signal (refer to text for details).

not a significant source of eddy activity over the region in the study period considered; however, the remote equatorial forcing plays a major role in controlling the eddy activity over the area.

B. Equatorial and Coastal Kelvin Wave

The BoB experiences two pairs of alternate upwelling and downwelling Kelvin waves (uKW and dKW, respectively) [14]. The first uKW occurs during January–April, and the second during August–September. The first dKW occurs during May-July, and the second during October–December. These uKWs and dKWs are generated in the EIO depending on the zonal wind over the region and propagate eastward. After reaching the eastern boundary of the Indian Ocean, some energy reflect as Rossby waves and the remaining propagate poleward as coastal Kelvin waves. In the BoB, these coastally trapped Kelvin waves of a given period radiate offshore Rossby waves at critical latitudes [15]. These radiated Rossby waves in the BoB manifest themselves as mesoscale eddies on the ocean surface. Among all the four types of Kelvin waves, the first uKW occurs during premonsoon [14] and has the ability to affect the premonsoon eddy activity. Hence, only the first uKW is analyzed in this letter.

To investigate the activity of the first uKW, 68 boxes, each with a dimension of 1°✖1°, are considered along the equator (starting from 80°E) and the boundary of the BoB up to the northern tip of Sri Lanka [Fig. 3(a)]. Fig. 3(b) shows time-box number plot of climatological SLA. It clearly shows the propagation of the first uKW during January–April in the eastern EIO and the coastal BoB. The first dKW starts in the month of May. Figs. 3(c) and (d) show the similar time-box number plots for premonsoon period of 2009 and 2012, respectively. It can be clearly discerned that in the first week of March 2009, the first dKW arises and extends up to Irrawaddy delta (box number 45), which inhibits the first uKW in the region. Though a signal of the first uKW is still there in the month of April, it is much weaker than that of February. In the case of 2012, the first uKW lasts only for a few days, during the month of February [Fig. 3(d)]. Hence, both the years 2009 and 2012 experience reduction in the first uKW activities in the EIO and the coastal BoB as well.

Moreover, it is noted that in all the three time-box number plots, the first discontinuity (patches of abrupt high/low SLA inside the negative SLA signal of the first uKW) is seen at box numbers 19–23, located at the Sumatra coast. This is due to the effect of boundary reflected Rossby waves, which are present there [16]. The second discontinuity is noticed at box numbers 29–34, which are located at the tip of Sumatra and the opening of the Malakka Strait. The possible reason for such discontinuities could be the effect of shallow bathymetry and boundary reflected Rossby waves. And the last and the third discontinuities are observed at box numbers 41–45, at the Irrawaddy delta. This may be due to bathymetry and westward radiation of Rossby waves [7]. It is interesting to note that strong radiation of Rossby waves was prominent from the Irrawaddy delta in years 2009 and 2012.

Furthermore, 2012 was a short-lived positive Indian Ocean Dipole (IOD) year [17]. Here, we examine whether this IOD has any effect on the first uKW in 2012 by analyzing zonal wind stress and SLA along the equator and SLA along the 5°S latitude. The time series plot of Dipole Mode Index (calculated using weekly TRMM Microwave Imager SST) shows that IOD starts developing toward the end of July, peaks during September and dissipates in October (see Fig. S2 in the Supplementary Material). During early August, strong easterly wind anomalies are observed in the EIO [see Fig. S3(a) in the Supplementary Material]. These winds force the uKW in the equator and produce upwelling at the eastern EIO (see Fig. S3(b) in the Supplementary Material). Meanwhile, a positive IOD pattern is developed in the EIO and negative (positive) SLA in the east (west) EIO. But, from the second half of August, the easterlies are replaced by the westerlies in the western EIO and sometimes in the central EIO [see Fig. S3(a) in the Supplementary Material]. These winds force dKW (positive SLA) in the EIO.

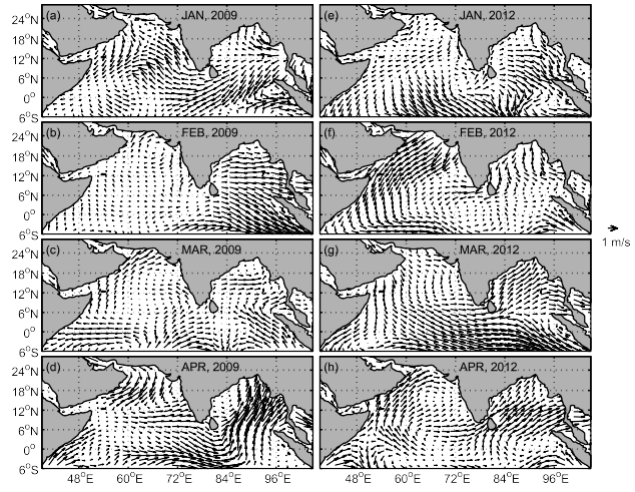

Fig. 4. Monthly anomaly of 10 m wind for January to April of two June ISM deficit years. (a)–(d) 2009. (e)–(h) 2012.

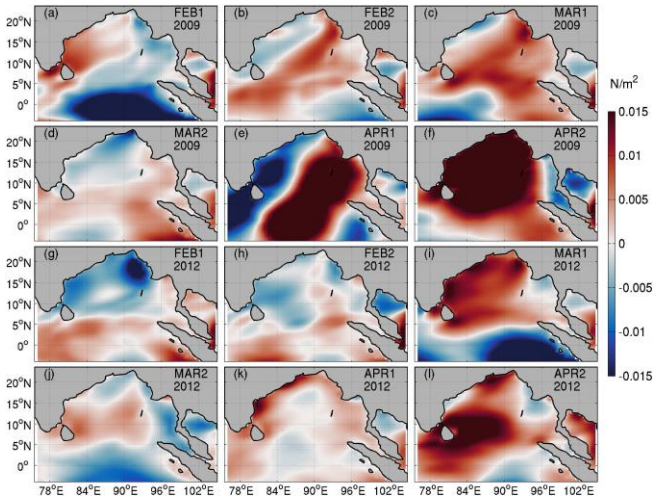

Fig. 5. Fortnightly meridional wind stress anomaly (in Nm^{-2}) for February–April of (a)–(f) 2009 and (g)–(l) 2012. FEB1 and FEB2 represent the first and second halves of February and likewise for the other months.

However, the easterlies in the eastern EIO force uKW in the EIO and downwelling Rossby wave (positive SLA) off the equator (see Fig. S3(c) in the Supplementary Material). By the beginning of November, westerlies are seen in both the eastern and western EIO, and the IOD signal completely disappears. During premonsoon period and the first half of June, strong westerlies are predominant in the EIO, though weak easterlies are present for some period in April. Due to the presence of strong westerlies, the dKW persists in the equatorial waveguide see Fig. S3(b) and (c) in the Supplementary (Material). No impact of positive IOD is seen on the first uKW of 2012.

C. Equatorial and Local Winds Over the BoB

The Kelvin waves in the EIO are mainly driven by the equatorial winds, and in the coastal waveguide of BoB, they get modified by the local winds. To examine the cause of the reduction in the first uKW, both the equatorial winds and local winds over the BoB are analyzed in detail. The easterly winds in the EIO force the uKWs, while the westerly wind bursts occurring during monsoon transition times force the dKWs [14]. Fig. 4 shows monthly wind anomalies for 2009 and 2012 from January to April. The wind anomalies during February are westerly in the EIO [Fig. 4(b)]. During April, they become westerly up to 87°E in the EIO and are southerly at the eastern boundary of EIO [Fig. 4(d)]. However, during March, wind anomalies are westerly in the longitude band of 70°E–84°E in the EIO; and southeasterly at the east of 84°E [Fig. 4(c)]. Hence, most of the time, the eastern EIO is dominated by westerly wind anomalies during the premonsoon period. These westerly wind anomalies produce anomalous coastal downwelling, which suppresses the first equatorial uKW. The signature of the first dKW appears in the eastern EIO during March 2009 [Fig. 3(c)]. In the case of 2012, the wind anomalies are mostly westerly during January, March, and April in most of the EIO and eastern EIO [Fig. 4 (right)]. The anomalies are very small during the month of February. These westerly wind anomalies produce anomalous equatorial downwelling and suppress the generation of the first equatorial uKW. As a consequence, a weak first equatorial uKW developed in the year 2012 and the first equatorial dKW appeared early [Fig. 3(d)].

Because of north–south alignment of the shoreline of the eastern BoB, the meridional wind stress mainly controls the coastal upwelling/downwelling in the eastern BoB, rather than its zonal component. Generally, from February to the first half of April, the climatological wind stress is negative/northerly (see Fig. S4 in the Supplementary Material). This produces coastal upwelling at the eastern rim of BoB, which supports the first uKW. However, the fortnightly anomalies of meridional wind stress during the second half of February to the end of April in 2009 are positive/southerly [Fig. 5(b)–(f)] at the eastern boundary of BoB. This causes anomalous coastal downwelling over the region. This coastal downwelling tries to nullify the effect of coastal upwelling induced by the first uKW, which is normally present during that time [Fig. 3(b)]. In other words, the coastal downwelling caused by southerly wind stress of 2009 blocks the first uKW to propagate northward. In the case of 2012, the meridional wind stress anomalies are southerly from March first half to end of April [Fig. 5(i)–(l)] resulting in the blocking of the first uKW in a similar manner to the year 2009. For this reason, termination of the first uKW accorded after the first week of March in 2012 over most of the eastern rim of the BoB (up to 47–50, the head bay) [Fig. 3(d)]. However, the signal of the first uKW lasted up to the first week of April beyond box number 50. The southerly wind stress anomaly produces anomalous coastal upwelling at the western rim of BoB, which favors the existing the first uKW signal beyond box number 50.

IV. Conclusion

This letter examines the premonsoon eddy and Kelvin wave activities in the northern BoB during the two June ISM deficit years 2009 and 2012, occurred in the recent warming hiatus period. This letter reveals that the cyclonic EKE is reduced by 35% and 50% during April–May of 2009 and 2012, respectively, whereas the cyclonic eddy area is reduced by

18% and 24%, respectively. Usually, the first uKW prevails in the BoB coast during February–April [Fig. 3(b)] [14], and radiates offshore upwelling Rossby waves [18]. This upwelling Rossby waves produce negative SLA, which are detected as cyclonic eddies in the interior of the bay [7]. The first uKW is found to be weak in 2009 and 2012. As a result, the cyclonic eddy activity is found to be reduced during April–May in the northern BoB in these years. The weakening of the first uKW in 2009 and 2012 is attributed to winds over both the eastern EIO and the eastern rim of BoB. The wind anomalies are noticed to be westerlies in the eastern EIO for most of the time in January–April of these years. This reduces the generation of the equatorial first uKW. Additionally, the meridional wind stress anomaly along the eastern boundary of BoB is found to be southerly during most of the time in March and April of these two years. This causes anomalous coastal downwelling and, hence, blocks the northward propagation of the first uKW along the BoB coastal waveguide. As a combined effect of these processes, the cyclonic eddy activity in the northern BoB is found to be reduced during April and May, which is nearly at one-month lag with the reduction of the first uKW in the coastal waveguide. Typical speed of the first baroclinic mode of Kelvin wave is 2.6–2.8 m/s [19]. It takes nearly 28 days to reach up to head bay from the equator. Hence, the one-month lag between the reduction of cyclonic eddy activity and the first uKW may be justified.

This letter reports the reduction of cyclonic eddy and the first uKW activities in the northern BoB in two June ISM deficit years during the warming hiatus period. Since the BoB is generally characterized by shallow mixed layer depth (25 m of annual average in the northern bay [20]), we believe that the reduced cyclonic eddy activity during premonsoon and the month of June of 2009 and 2012 could affect the vertical mixing in the upper ocean surface, thus causing redistribution of heat in the northern bay. The features of mesoscale eddy and Kelvin wave activities in the premonsoon period of ISM deficit years could be very useful for investigating upper ocean mixing processes in the BoB and supplement our current understanding of ISM deficit. A detailed investigation of air–sea interaction and heat budget over the region will provide valuable insight into the interaction between eddy activities over the BoB and June ISM deficit.

ACKNOWLEDGMENT

The authors would like to thank Prof. B. N. Goswami and Dr. F. Durand for their valuable suggestions during this letter. The altimeter products were produced by Ssalto/Duacs and distributed by Aviso with support from Cnes. MERRA data used in this letter have been provided by the Global Modeling and Assimilation Office at the NASA Goddard Space Flight Center through the NASA Goddard Earth Sciences Data and Information Services Center online archive.

REFERENCES

[1] K. Li *et al.*, "Possible role of pre-monsoon sea surface warming in driving the summer monsoon onset over the Bay of Bengal," *Climate Dyn.*, vol. 47, nos. 3–4, pp. 753–763, 2016.

[2] S. K. Jadhav and A. A. Munot, "Warming SST of Bay of Bengal and decrease in formation of cyclonic disturbances over the Indian region during southwest monsoon season," *Theor. Appl. Climatol.*, vol. 96, nos. 3–4, pp. 327–336, 2009.

[3] B. N. Goswami, S. A. Rao, D. Sengupta, and S. Chakravorty, "Monsoons to mixing in the Bay of Bengal: Multiscale air-sea interactions and monsoon predictability," *Oceanography*, vol. 29, no. 2, pp. 18–27, 2016.

[4] J. Isern-Fontanet, J. Font, E. García-Ladona, M. Emelianov, C. Millot, and I. Taupier-Letage, "Spatial structure of anticyclonic eddies in the Algerian basin (Mediterranean Sea) analyzed using the Okubo–Weiss parameter," *Deep Sea Res. II, Topical Stud. Oceanogr.*, vol. 51, nos. 25–26, pp. 3009–3028, 2004.

[5] I. Frenger, N. Gruber, R. Knutti, and M. Münnich, "Imprint of Southern Ocean eddies on winds, clouds and rainfall," *Nature Geosci.*, vol. 6, no. 8, pp. 608–612, 2013.

[6] P. Sreenivas, C. Gnanaseelan, and K. V. S. R. Prasad, "Influence of El Nino and Indian Ocean Dipole on sea level variability in the Bay of Bengal," *Global Planetary Change*, vols. 80–81, pp. 215–225, Jan. 2012.

[7] X. Cheng, S.-P. Xie, J. P. McCreary, Y. Qi, and Y. Du, "Intraseasonal variability of sea surface height in the Bay of Bengal," *J. Geophys. Res.*, vol. 118, no. 2, pp. 816–830, 2013.

[8] H. Ueda *et al.*, "Combined effects of recent Pacific cooling and Indian Ocean warming on the Asian monsoon," *Nature Commun.*, vol. 6, Nov. 2015, Art. no. 8854.

[9] S.-K. Lee, W. Park, M. O. Baringer, A. L. Gordon, B. Huber, and Y. Liu, "Pacific origin of the abrupt increase in Indian Ocean heat content during the warming hiatus," *Nature Geosci.*, vol. 8, no. 6, pp. 445–449, 2015.

[10] A. Okubo, "Horizontal dispersion of floatable particles in the vicinity of velocity singularities such as convergences," *Deep Sea Res. Oceanogr. Abstracts*, vol. 17, no. 3, pp. 445–454, 1970.

[11] S. A. Henson and A. C. Thomas, "A census of oceanic anticyclonic eddies in the Gulf of Alaska," *Deep Sea Res. I, Oceanogr. Res. Papers*, vol. 55, no. 2, pp. 163–176, 2008.

[12] S. A. Thorpe, *An Introduction to Ocean Turbulence*. Cambridge, U.K.: Cambridge Univ. Press, 2007.

[13] U. Frisch, *Turbulence: The Legacy of A. N. Kolmogorov*. Cambridge, U.K.: Cambridge Univ. Press, 1995.

[14] R. R. Rao, M. S. G. Kumar, M. Ravichandran, A. R. Rao, V. V. Gopalakrishna, and P. Thadathil, "Interannual variability of Kelvin wave propagation in the wave guides of the equatorial Indian Ocean, the coastal Bay of Bengal and the southeastern Arabian Sea during 1993–2006," *Deep Sea Res. I, Oceanogr. Res. Papers*, vol. 57, no. 1, pp. 1–13, 2010.

[15] A. J. Clarke and C. Shi, "Critical frequencies at ocean boundaries," *J. Geophys. Res., Oceans*, vol. 96, no. C6, pp. 10731–10738, 1991.

[16] I. Iskandar, M. Irfan, and F. Saymsuddin, "Why was the 2008 Indian Ocean Dipole a short-lived event?" *Ocean Sci. J.*, vol. 48, no. 2, pp. 149–160, 2013.

[17] N. H. Saji, B. N. Goswami, P. N. Vinayachandran, and T. Yamagata, "A dipole mode in the tropical Indian Ocean," *Nature*, vol. 401, no. 6751, pp. 360–363, 1999.

[18] S. S. C. Shenoi, D. Shankar, and S. R. Shetye, "On the sea surface temperature high in the Lakshadweep Sea before the onset of the southwest monsoon," *J. Geophys. Res., Oceans*, vol. 104, no. C7, pp. 15703–15712, 1999.

[19] D. B. Chelton, R. A. Deszoeke, M. G. Schlax, K. El Naggar, and N. Siwertz, "Geographical variability of the first baroclinic Rossby radius of deformation," *J. Phys. Oceanograph.*, vol. 28, pp. 433–460, Mar. 1998.

[20] T. Pankajakshan, P. M. Muraleedharan, R. R. Rao, Y. K. Somayajulu, G. V. Reddy, and C. Revichandran, "Observed seasonal variability of barrier layer in the Bay of Bengal," *J. Geophys. Res., Oceans*, vol. 112, no. C2, p. C02009, 2007.